Chemical Science

ROYAL SOCIETY OF CHEMISTRY

EDGE ARTICLE

View Article Online
View Journal | View Issue

Cite this: *Chem. Sci.*, 2023, **14**, 3676

All publication charges for this article have been paid for by the Royal Society of Chemistry

Received 7th November 2022
Accepted 27th February 2023

DOI: 10.1039/d2sc06131g

rsc.li/chemical-science

Atroposelective brominations to access chiral biaryl scaffolds using high-valent Pd-catalysis†

Sif T. Linde, Vasco Corti, Vibeke H. Lauridsen, Johannes N. Lamhauge, Karl Anker Jørgensen and Nomaan M. Rezayee *

Compounds featuring atropisomerism are ubiquitous in natural products, therapeutics, advanced materials, and asymmetric synthesis. However, stereoselective preparation of these compounds presents many synthetic challenges. This article introduces streamlined access to a versatile chiral biaryl template through C–H halogenation reactions employing high-valent Pd catalysis in combination with chiral transient directing groups. This methodology is highly scalable, insensitive to moisture and air, and proceeds, in select cases, with Pd-loadings as low as 1 mol%. Chiral mono-brominated, dibrominated, and bromochloro biaryls are prepared in high yield and excellent stereoselectivity. These serve as remarkable building blocks bearing orthogonal synthetic handles for a gamut of reactions. Empirical studies elucidated regioselective C–H activation to be predicated on the oxidation state of Pd and diverging site-halogenation to result from cooperative effects of Pd and oxidant.

Atropisomers are a subset of axially chiral compounds bearing restricted rotation about a σ-bond pivot—leading to isolable conformers exhibiting molecular asymmetry.[1,2] Within the various classes of atropisomers, biaryls are distinguished as privileged scaffolds due to their salient contributions to the field of asymmetric catalysis found in phosphoric acid-, Brønsted base-, phase-transfer-, aldehyde-, H-bond-, Cu–H-catalysis *etc.*[3] Consequently, significant efforts have been devoted to streamline access to novel chiral scaffolds.

Among the various methods to prepare atropisomers, the development of transition metal catalyzed asymmetric C–H functionalizations of biaryls through an enantioconvergent process has manifested into a powerful strategy.[4–8] These hinge on the combined effects of directing groups/chiral auxiliaries, chiral ancillary ligands, and metal catalysts. Within this frame, elegant directing group-assisted approaches have been developed relying on either "catalyst control"[9–11] or "substrate-control"[12–14] for the stereoinduction. However, these methods exhibit key limitations that hinder broad application. For instance, additional steps are necessary for the stoichiometric installation and removal of optically pure (substrate-control) or achiral (catalyst-control) directing groups. These complicate syntheses and often lead to harsh conditions incompatible with structurally complex compounds.[15] An attractive strategy that circumvents these limitations is the use of chiral transient directing groups (cTDGs).[15–18]

Significant progress has been made employing cTDGs for the stereoselective preparation of atropisomers employing Pd-catalysis. A seminal contribution by the Shi group identified the chiral amino acids as a competent cTDG to reversibly condense with the carbonyl moiety of benzaldehyde derivatives (Scheme 1, precedent).[19] The resulting *in situ* generated chiral imine directing group underwent the Fujiwara–Moritani reaction and demonstrated high proficiency for stereoinduction yielding the C–H olefinated biaryl with >99% enantiomeric excess (ee). This strategy has proven general and robust leading

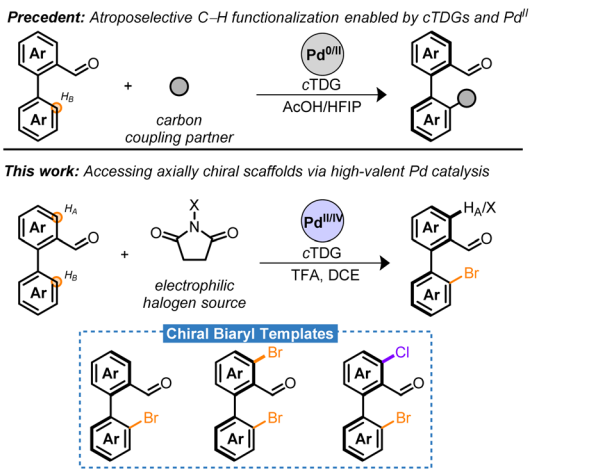

Scheme 1 Pd-catalyzed atroposelective C–H functionalizations employing cTDGs.

Department of Chemistry, Aarhus University, DK-8000 Aarhus C, Denmark. E-mail: nmr@chem.au.dk

† Electronic supplementary information (ESI) available. CCDC 2169123 and 2168153. For ESI and crystallographic data in CIF or other electronic format see DOI: https://doi.org/10.1039/d2sc06131g

to C–H alkynylations,[20,21] allylations,[22] naphthylations,[23] and alkylations[24] with chiral amino acids playing an essential role in the $Pd^{0/II}$ cycle. Ackermann and co-workers have adapted this approach to electro-chemical setups with comparable success.[25] Despite these advances, to date, the cTDG C–H functionalization reaction has been nearly exclusively limited to C–C bond formation[26,27] and predominantly employs a $Pd^{0/II}$ cycle.[6,15,28]

This article describes the atroposelective halogenation of C–H bonds by combining cTDG with high-valent Pd catalysis. Notably, reductive eliminations to forge C–X bonds are typically not feasible from Pd^{II} in a catalytic setting.[29,30] Chiral dihalogenated and monohalogenated biaryls are prepared in moderate to excellent yield with, generally, excellent enantioselectivity (Scheme 1, this work). The presented method is insensitive to moisture and air, is highly scalable, and, in select cases, proceeds with Pd-loadings as low as 1 mol%. The resulting chiral bromobenzaldehyde derivatives serve as remarkable synthetic templates bearing two orthogonal handles for diversification adjacent to the axis of asymmetry. Methodologies for synthetic elaboration of aryl bromides and aldehydes are pervasive in literature. Harnessing these functional groups may bridge access to a multitude of chiral compounds that would otherwise necessitate extensive synthetic effort or the advent of new methodologies. The versatility of the chiral templates is highlighted in a series of transformations to forge C–B, C–C, C–N, C–O, C–F, and C–P bonds in a stereoretentive manner. Finally, a rare example of Pd-catalyzed oxidant-dependent regiocontrol was harnessed into telescoping reactions to furnish chiral bromochloro biaryls.

Biaryl **1a**, in conjunction with cTDG1 and the halogenation reagent, NBS **2a**, were selected to begin our investigation into the Pd-catalyzed reaction (Table 1). Initial attempts led to complex reaction mixtures; however, we were encouraged by the viability of the reaction and additional NBS was added. Upon the addition of 2.1 equivalents of NBS, the mixture of products coalesced into a single, di-brominated product, **3a**. Investigations were undertaken to identify optimal reaction parameters. To our surprise 1,1,1,3,3,3-hexafluoro-propan-2-ol (HFIP),[19,24,31,32] the typical solvent used with cTDGs, did not lead to marked improvement (entry 1). Instead, a survey (see ESI†) of solvents identified 1,2-dichloroethane (DCE) to provide the desired product in 48% yield as determined by NMR spectroscopy with >99% ee (entry 2) when employing cTDG1 and 10 equivalents of trifluoracetic acid (TFA).[33] A suite of other amino acids and *tert*-leucine derived compounds (cTDGs 2–6) led to diminished yields and enantioselectivity (entries 2–7)—securing the use of commercially available L-*tert*-leucine (cTDG1). Notably, the addition of TFA was essential for the reaction to proceed (entry 8). Finally, a brief evaluation of additives found Ag_2CO_3 to improve yields to 84% (entries 9 and 10).[34]

With the optimized conditions in hand, we next focused our attention on the Pd-catalyzed bromination of other biaryl compounds. The resulting enantioconvergent strategy proved universal—accommodating diverse steric profiles on the bottom ring (**3b–m**), top ring (**3c–d**, and **3h–p**) and electronic parameters (**3e–g**, **3l**, and **3p**), in moderate to excellent yield and

Table 1 Optimization of the atroposelective bromination of **1a** [a]

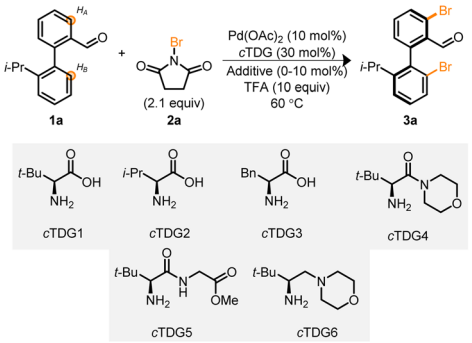

Entry	cTDG	Solvent	Additive	Yield (%)	ee (%)
1	cTDG1	HFIP	—	0	—
2	cTDG1	DCE	—	48	>99
3	cTDG2	DCE	—	22	94
4	cTDG3	DCE	—	4	nd
5	cTDG4	DCE	—	42	85
6	cTDG5	DCE	—	8	nd
7	cTDG6	DCE	—	0	—
8[b]	cTDG1	DCE	—	0	—
9	cTDG1	DCE	AgTFA	64	>99
10	cTDG1	DCE	Ag_2CO_3	84	>99

[a] Conditions: 0.1 mmol **1a**, 1.0 mL solvent, 0.1 equiv. of additive, 16 h. Yield determined by ^{1}H NMR, ee determined by UPC^2. [b] TFA omitted.

excellent enantioselectivity (Table 2). In the context of compounds **3g** and **3h**, poor mass balance was observed. Notably, the atroposelective halogenation of the electron-rich biaryl **1l** led to the tribrominated product **3l** in high yield and enantioselectivity. Previous works in the C–H halogenation of electron-rich arenes have revealed an uncatalyzed, background pathway consistent with the regioselectivity observed in **3l**.[35]

These products serve as versatile, catalytically-relevant scaffolds typified in **3p** which resembles a hybrid among the core structures of BINAP and SEGPHOS. Notably, the installation of the Br-functional group is compatible with other synthetic handles such as Cl (**3g**) and pseudohalides (**3h–k**) directly adjacent to the axis of chirality. This allows for a myriad of orthogonal synthetic manipulations with three distinct sites for synthetic diversification flanking a pre-set stereogenic axis.

Several tactics can be taken to attenuate the extent of bromination in these systems to achieve monohalogenation (Table 2, monobromination). For instance: (1) the incorporation of a substituent at the H_A-position (**4q–v**), (2) sterically occlude the undesired site (**4w**), (3) electronically deactivate the reactive site (**4x**), and (4) decrease the Pd loading to 1 mol% (**4y**, **4i**, **4z**, **4a**, and **4b**). Of particular significance is compound **4ϕ** which provides a vector for the preparation of libraries of chiral terphenyls with high enantiopurity. Among the strategies, the latter approach necessitated delicate refinement and reoptimization (see ESI†). Nonetheless, we were pleased to find that 1 mol% of $Pd(OAc)_2$ was sufficient to promote the reaction in moderate to good yield and high enantioselectivity. The

Table 2 Scope of atroposelective C–H bromination of biaryls *via* high-valent Pd-catalysis[a]

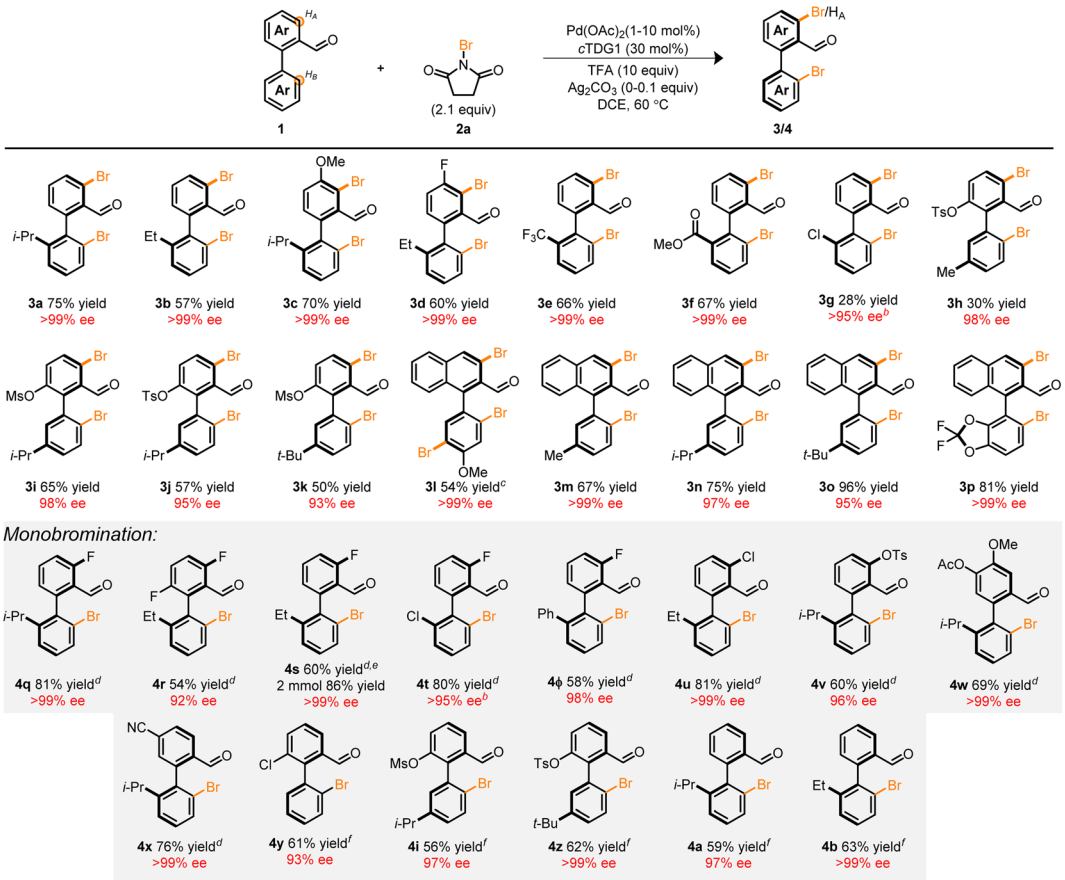

[a] Conditions: 0.1 mmol **1**, 1.0 mL DCE, 0.1 equiv. Ag_2CO_3, 16 h. Yield are isolated yields, ee determined by UPC[2]. [b] ee determined by ^{1}H NMR employing (*R*)-2-methyl-2-propanesulfinamide. [c] 3.1 equiv. of **2a**. [d] 1.1 equiv. of **2a**. [e] 2.0 mmol scale, 20 mL DCE. [f] 1.0 mol% $Pd(OAc)_2$, 1.8 equiv. **2a**, and Ag_2CO_3 omitted.

influence of palladium loading on iteroselectivity may potentially arise from competitive hydrolysis, condensation, and ligand substitution of unfunctionalized starting material prior to a second C–H functionalization event (see ESI†). Furthermore, a two mmol scale-up reaction of **4s** demonstrated the scalability of the transformation leading to an improved yield of 86% and >99% ee. The fidelity of the stereogenic axis for a variety of halogenated biaryls was interrogated experimentally and computationally with half-lives ranging from 92.3–114.9 h at 180 °C (see ESI†).

The brominated benzaldehyde derivatives behave as chiral templates for the construction of synthetically valuable biaryls through functionalization of either the aryl halide or aldehyde motif. Together, the orthogonal reactivity of the synthetic handles allows for the introduction of an array of functional groups. Summarized in Scheme 2 is a tableau of reactions to derivatize compounds **4q**, **4s**, or **4s′**. The acetal protected **4s′** was amenable to a variety of C–C bond forming reactions such as carboxylation *via* lithiation, the Suzuki–Miyuara coupling, and Pd-catalyzed cyanation in a stereoretentive manner (Scheme 2a–c). In addition, heteroatoms can also be installed through established cross-coupling methodologies to construct, C–B, C–N, and C–P[36] bonds adjacent to the stereogenic axis (Scheme 2d–f). Atroposelective methods to form these bonds through other means have remained elusive. Functionalization of the aldehyde moiety introduces a complementary avenue for diversification without erosion of the optical purity through reductive amination, deoxyfluorination, Baeyer–Villiger oxidation, and oxazoline forming reactions (Scheme 2g–j). An attractive prospect of the stereospecific Baeyer–Villiger reaction is the access to phenols which may be conveniently converted into a pseudohalide. In addition, the dibrominated benzaldehyde products exhibited preference for regioselective Suzuki–Miyuara couplings at the H_A-site, allowing for potential iterative cross-couplings (see ESI†).

Attempts to extend this methodology to other halogens proved unfruitful[37–39] despite precedent for atroposelective iodinations employing chiral auxiliaries[13] or chiral ancillary ligands.[10] However, through our studies, a rare example of Pd-mediated oxidant dependent regiocontrol was identified. Unlike NBS, NCS **2b** exclusively functionalized H_A. This feature was recruited into telescoping reactions depicted in Table 3. At

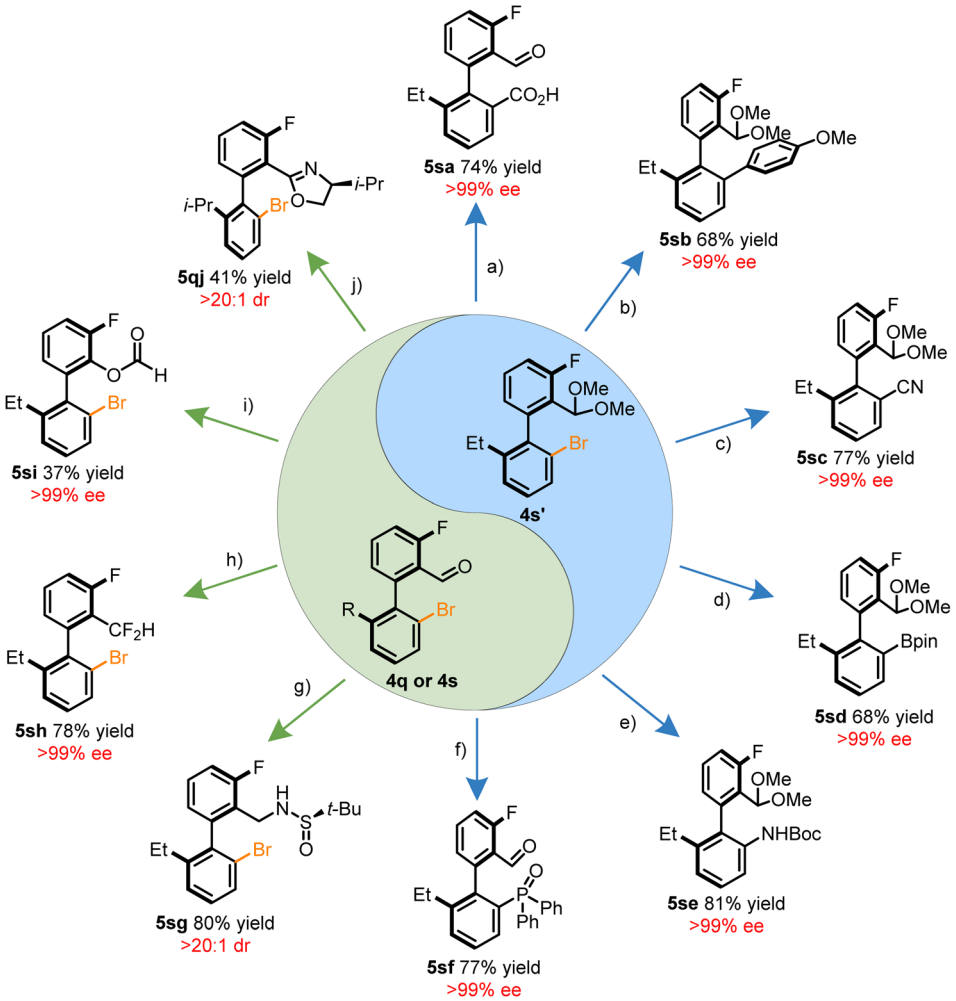

Scheme 2 Application of chiral biaryl templates to access novel chiral scaffolds. (a) *tert*-BuLi (2.0 equiv.), then CO_2, −90 °C. (b) *p*-Methoxyphenylboronic acid (1.5 equiv.), Pd(XPhos)-G4 (2 mol%), K_3PO_4 (2 equiv.). rt. (c) $Na_4[Fe(CN)_6]\cdot 10H_2O$ (0.5 equiv.), $Pd_2(dba)_3$ (2.5 mol%), XPhos (20 mol%), KOAc (12.5 mol%), 100 °C. (d) B_2Pin_2 (4.0 equiv.), Pd(dppf)Cl_2 (10 mol%), KOAc (5.0 equiv.), 90 °C. (e) $BocNH_2$ (2.0 equiv.), Pd$(OAc)_2$ (10 mol%), XPhos (30 mol%), Cs_2CO_3 (1.4 equiv.), 100 °C. (f) $Ph_2P(O)H$ (2.0 equiv.), Pd$(OAc)_2$ (20 mol%), dppb (30 mol%), DIPEA (4.8 equiv.), 120 °C. (g) (*R*)-2-Methyl-2-propanesulfinamide (1.2 equiv.), Ti(*i*-PrO)$_4$ (4.0 equiv.), 40 °C then $NaBH_4$ (4.0 equiv.), rt. (h) DAST (3.5 equiv.), rt. (i) *m*CPBA (3.3 equiv.) 0 °C to rt. (j) L-Valinol (1.0 equiv.), then NBS (1.0 equiv.), rt.

the onset, Pd, cTDG1, in conjunction with NCS, selectively furnished the mono, *ortho*-chlorinated product despite the vast excess in NCS. Subsequent addition of NBS installed Br at the H_B-position, providing a chiral, mixed halogenated biaryl template with complete stereo- and regiocontrol. Remarkably, no reaction took place in the absence of Pd and cTDG1; indicating a cooperative effect among oxidant and Pd. Products arising from mixed chloro- and bromo-halogens provide synthetically valuable platforms allowing for chemodivergent cross-coupling reactions.[40] This allows for facile initial tailoring at H_B and subsequent refinement at H_A. Notably, the resulting mixed halogen products deliver a complementary pathway for divergent iterative cross-couplings to the dibrominated products **4** (see ESI†). While a host of substrates are amenable to these telescoping reactions, Table 3 provides a brief survey.

Based on the atypical circumstance of functionalization proceeding at chemically distinct sites,[41,42] we were interested in gaining insight into the origin of the regiodivergent C–H activation. Previous atroposelective strategies employing TDGs in a $Pd^{0/II}$ manifold afforded exclusive functionalization of H_B with no indications of competitive H_A- or di-functionalization despite employing the same cTDG and Pd source.[19–24,31,32] However, a distinguishing facet from prior works is the implementation of a high-valent Pd manifold.[29,30,35,37] To interrogate whether the oxidation state of Pd was the root of regiocontrol, empirical studies were undertaken. Depicted in Scheme 3 is a pair of deuterium labeling experiments evaluating the reversible C–H functionalization(s) under contrasting reaction conditions. In Scheme 3a, conditions suitable to access high-valent Pd catalysis are achieved employing NCS and TFA-d. The resulting monochlorinated biaryl product **7a–d**, exhibited selective chlorination at H_A and 67% deuterium incorporation at H_B. These results indicate that under oxidative reaction conditions, both sites undergo C–H activation, however, when

Table 3 Site selective divergent C–H halogenation[a]

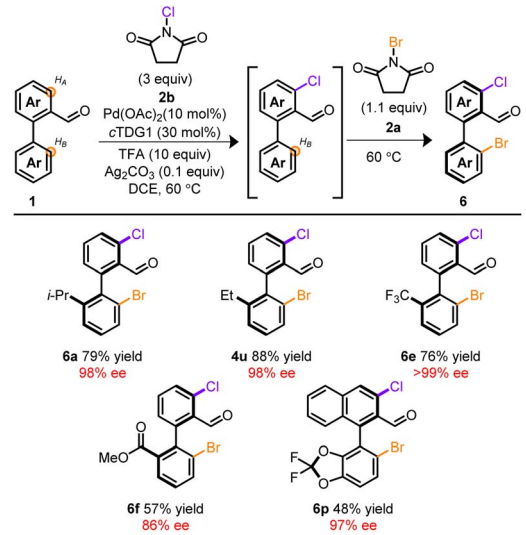

[a] Conditions: 0.1 mmol **1**, 1.0 mL DCE, 48 h then 16 h.

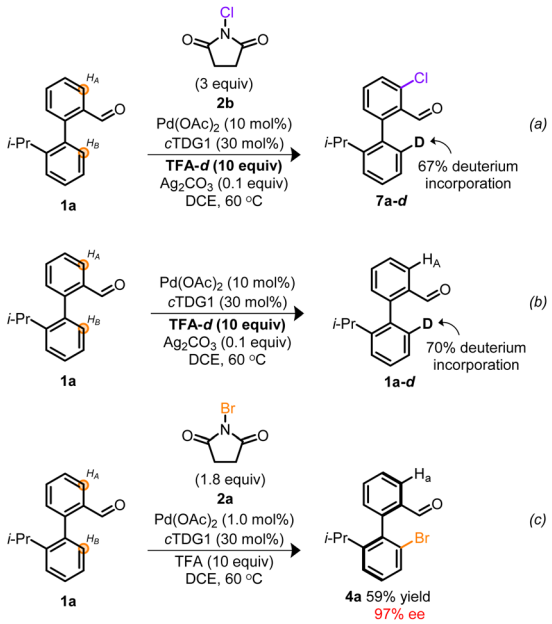

Scheme 3 (a) Deuterium labeling experiment under oxidative conditions employing NCS. (b) Deuterium labeling experiment at Pd^{II} and in the absence of oxidant. (c) Empirical result from Table 2 **4a**.

employing NCS, chlorination exclusively occurs vicinal to the aldehyde. Conversely, Scheme 3b reveals the reversible C–H activation, in the absence of exogeneous oxidant, to solely proceed at H_B—consistent with previous atroposelective reports at Pd^{II}.[19–24,31,32] Taken together, Scheme 3 suggests a variance in site selectivity for C–H activation to be predicated on the oxidation state of Pd.[43] Empirical distinctions between NCS and NBS suggest a divergence in site halogenation. NCS initially functionalizes H_A (Scheme 3a) whereas NBS exclusively halogenates H_B (Scheme 3c). The origin of this divergence remains unclear. Nevertheless, this marks a rare example of Pd-catalyzed oxidant-dependent regiocontrol.

In summary, this article describes the first example of an atroposelective methodology to form C–X bonds using high-valent Pd-catalysis in conjunction with cTDGs. These transformations were achieved with Pd loadings ranging from 10 mol% to as low as 1 mol%. The resulting mono- and dihalogenated chiral biaryls were formed with excellent stereoselectivity and proved to be outstanding building blocks to undergo a gamut of stereoretentive transformations. Remarkably, empirical C–H activation studies reveal variances in regioselectivity based on the oxidation state of Pd and diverging sites of halogenation based on the oxidant. We anticipate this methodology to spur developments into novel asymmetric ligands and catalysts.

Data availability

All experimental and characterization data, as well as NMR spectra are available in the ESI.† Crystallographic data for compounds **3c** and **6p** have been deposited in the Cambridge Crystallographic Data Centre under accession number CCDC 2169123 (**3c**) and 2168153 (**6p**).

Author contributions

N. M. R. conceived and supervised the work. S. T. L. optimized and identified the initial reaction conditions. S. T. L., V. C., and N. M. R. designed and executed the experiments. V. H. L. obtained the initial reaction result. J. N. L. performed experimental edits requested in the revision process. N. M. R., S. T. L., V. C., and K. A. J. contributed to writing and editing the manuscript. All authors agreed on the final version of the manuscript.

Conflicts of interest

There are no conflicts to declare.

Acknowledgements

K. A. J. thanks Villum Investigator grant (no. 25867), the Carlsberg Foundation "Semper Ardens", FNU and Aarhus University.

Notes and references

1 E. V. D. Anslyn and A. Dennis, *Modern Physical Organic Chemistry*, University Science Books, Herndon, VA, 2005.
2 G. Bringmann, A. J. Price Mortimer, P. A. Keller, M. J. Gresser, J. Garner and M. Breuning, *Angew. Chem., Int. Ed.*, 2005, **44**, 5384–5427.
3 J. K. Cheng, S.-H. Xiang, S. Li, L. Ye and B. Tan, *Chem. Rev.*, 2021, **121**, 4805–4902.
4 Q. Wang, Z.-J. Cai, C.-X. Liu, Q. Gu and S.-L. You, *J. Am. Chem. Soc.*, 2019, **141**, 9504–9510.

5 Q. Wang, W.-W. Zhang, H. Song, J. Wang, C. Zheng, Q. Gu and S.-L. You, *J. Am. Chem. Soc.*, 2020, **142**, 15678–15685.
6 C.-X. Liu, W.-W. Zhang, S.-Y. Yin, Q. Gu and S.-L. You, *J. Am. Chem. Soc.*, 2021, **143**, 14025–14040.
7 J. Frey, X. Hou and L. Ackermann, *Chem. Sci.*, 2022, **13**, 2729–2734.
8 Y. Li, Y.-C. Liou, X. Chen and L. Ackermann, *Chem. Sci.*, 2022, **13**, 4088–4094.
9 F. Kakiuchi, P. Le Gendre, A. Yamada, H. Ohtaki and S. Murai, *Tetrahedron: Asymmetry*, 2000, **11**, 2647–2651.
10 D.-W. Gao, Q. Gu and S.-L. You, *ACS Catal.*, 2014, **4**, 2741–2745.
11 Y.-N. Ma, H.-Y. Zhang and S.-D. Yang, *Org. Lett.*, 2015, **17**, 2034–2037.
12 T. Wesch, F. R. Leroux and F. Colobert, *Adv. Synth. Catal.*, 2013, **355**, 2139–2144.
13 C. K. Hazra, Q. Dherbassy, J. Wencel-Delord and F. Colobert, *Angew. Chem., Int. Ed.*, 2014, **53**, 13871–13875.
14 Q. Dherbassy, J.-P. Djukic, J. Wencel-Delord and F. Colobert, *Angew. Chem., Int. Ed.*, 2018, **57**, 4668–4672.
15 G. Liao, T. Zhang, Z.-K. Lin and B.-F. Shi, *Angew. Chem., Int. Ed.*, 2020, **59**, 19773–19786.
16 M. I. Lapuh, S. Mazeh and T. Besset, *ACS Catal.*, 2020, **10**, 12898–12919.
17 C. Jacob, B. U. W. Maes and G. Evano, *Chem. - Eur. J.*, 2021, **27**, 13899–13952.
18 P. Gandeepan and L. Ackermann, *Chem*, 2018, **4**, 199–222.
19 Q. J. Yao, S. Zhang, B. B. Zhan and B. F. Shi, *Angew. Chem., Int. Ed.*, 2017, **56**, 6617–6621.
20 S. Zhang, Q.-J. Yao, G. Liao, X. Li, H. Li, H.-M. Chen, X. Hong and B.-F. Shi, *ACS Catal.*, 2019, **9**, 1956–1961.
21 G. Liao, Q.-J. Yao, Z.-Z. Zhang, Y.-J. Wu, D.-Y. Huang and B.-F. Shi, *Angew. Chem., Int. Ed.*, 2018, **57**, 3661–3665.
22 H.-M. Chen, S. Zhang, G. Liao, Q.-J. Yao, X.-T. Xu, K. Zhang and B.-F. Shi, *Organometallics*, 2019, **38**, 4022–4028.
23 G. Liao, H.-M. Chen, Y.-N. Xia, B. Li, Q.-J. Yao and B.-F. Shi, *Angew. Chem., Int. Ed.*, 2019, **58**, 11464–11468.
24 H.-M. Chen, G. Liao, C.-K. Xu, Q.-J. Yao, S. Zhang and B.-F. Shi, *CCS Chem.*, 2021, **3**, 455–465.
25 U. Dhawa, C. Tian, T. Wdowik, J. C. A. Oliveira, J. Hao and L. Ackermann, *Angew. Chem., Int. Ed.*, 2020, **59**, 13451–13457.
26 Q. Gao, C. Wu, S. Deng, L. Li, Z.-S. Liu, Y. Hua, J. Ye, C. Liu, H.-G. Cheng, H. Cong, Y. Jiao and Q. Zhou, *J. Am. Chem. Soc.*, 2021, **143**, 7253–7260.
27 Z.-S. Liu, Y. Hua, Q. Gao, Y. Ma, H. Tang, Y. Shang, H.-G. Cheng and Q. Zhou, *Nat. Catal.*, 2020, **3**, 727–733.
28 J. Zhang, J. Fan, Y. Wu, Z. Guo, J. Wu and M. Xie, *Org. Lett.*, 2022, **24**, 5143–5148.
29 A. H. Roy and J. F. Hartwig, *Organometallics*, 2004, **23**, 1533–1541.
30 A. J. Hickman and M. S. Sanford, *Nature*, 2012, **484**, 177–185.
31 J. Zhang, Q. Xu, J. Wu, J. Fan and M. Xie, *Org. Lett.*, 2019, **21**, 6361–6365.
32 J. Fan, Q.-J. Yao, Y.-H. Liu, G. Liao, S. Zhang and B.-F. Shi, *Org. Lett.*, 2019, **21**, 3352–3356.
33 X.-H. Liu, H. Park, J.-H. Hu, Y. Hu, Q.-L. Zhang, B.-L. Wang, B. Sun, K.-S. Yeung, F.-L. Zhang and J.-Q. Yu, *J. Am. Chem. Soc.*, 2017, **139**, 888–896.
34 T. Bhattacharya, S. Dutta and D. Maiti, *ACS Catal.*, 2021, **11**, 9702–9714.
35 D. Kalyani, A. R. Dick, W. Q. Anani and M. S. Sanford, *Tetrahedron*, 2006, **62**, 11483–11498.
36 Q.-Y. Zhao and M. Shi, *Tetrahedron*, 2011, **67**, 3724–3732.
37 D. Kalyani, A. R. Dick, W. Q. Anani and M. S. Sanford, *Org. Lett.*, 2006, **8**, 2523–2526.
38 D. C. Powers and T. Ritter, *Nat. Chem.*, 2009, **1**, 302–309.
39 D. C. Powers, D. Y. Xiao, M. A. L. Geibel and T. Ritter, *J. Am. Chem. Soc.*, 2010, **132**, 14530–14536.
40 E. K. Reeves, E. D. Entz and S. R. Neufeldt, *Chem. - Eur. J.*, 2021, **27**, 6161–6177.
41 S. R. Neufeldt and M. S. Sanford, *Acc. Chem. Res.*, 2012, **45**, 936–946.
42 G. Meng, N. Y. S. Lam, E. L. Lucas, T. G. Saint-Denis, P. Verma, N. Chekshin and J.-Q. Yu, *J. Am. Chem. Soc.*, 2020, **142**, 10571–10591.
43 J. M. Racowski, N. D. Ball and M. S. Sanford, *J. Am. Chem. Soc.*, 2011, **133**, 18022–18025.